AD-A253 484

(2)

REPORT DOCUMENTATION PAGE

DTIC ELECTE JUL 24 1992 S D

Unclassified 2a. SECURITY CLASSIFICATION AUTHORITY	1b. RESTRICTIVE MARKINGS
2b. DECLASSIFICATION/DOWNGRADING SCHEDULE	3. DISTRIBUTION/AVAILABILITY OF REPORT Approved for Public Release, distribution unlimited
4. PERFORMING ORGANIZATION REPORT NUMBER(S)	5. MONITORING ORGANIZATION REPORT NUMBER(S) AFOSR-TR- 2 0089
6a. NAME OF PERFORMING ORGANIZATION Department of Materials Science and Engineering 6b. OFFICE SYMBOL (If applicable)	7a. NAME OF MONITORING ORGANIZATION Same as 8a
6c. ADDRESS (City, State and ZIP Code) 77 Massachusetts Ave. Cambridge, MA 02139	7b. ADDRESS (City, State and ZIP Code) Same as 8c
8a. NAME OF FUNDING/SPONSORING ORGANIZATION Air Force Office of Scientific Research 8b. OFFICE SYMBOL (If applicable) NE	9. PROCUREMENT INSTRUMENT IDENTIFICATION NUMBER AFOSR 85-0154
8c. ADDRESS (City, State and ZIP Code) Building 410 Bolling Air Force Base, DC 20332	10. SOURCE OF FUNDING NOS. PROGRAM ELEMENT NO. 61102F; PROJECT NO. 3306; TASK NO. B1; WORK UNIT NO.
11. TITLE (Include Security Classification) Post-Nucleation Heteroepitaxy ...	
12. PERSONAL AUTHOR(S) Carl V. Thompson	
13a. TYPE OF REPORT Final 13b. TIME COVERED FROM 10/88 TO 10/91	14. DATE OF REPORT (Yr., Mo., Day) March 6, 1992 15. PAGE COUNT
16. SUPPLEMENTARY NOTATION	
17. COSATI CODES: FIELD / GROUP / SUB. GR. 18. SUBJECT TERMS (Continue on reverse if necessary and identify by block number)	

19. ABSTRACT (Continue on reverse if necessary and identify by block number)

We have investigated the evolution of thin film structures in the earlier stages of film growth. We have also investigated epitaxial grain growth as a new method for obtaining epitaxial films in poorly lattice-matched systems. We have shown that the As_4 to Ga flux ratio can greatly affect the growth morphology of epitaxial GaAs islands on silicon, and that lower than conventinally used ratios can lead to initial layers and thicker films wit greatly improved electronic properties. We have also demonstrated that grain growth in polycrystalline films on single crystal substrates can lead to very thin epitaxial films of higher quality than can be obtained by other techniques. We have also shown that epitaxial grain growth can be used to establish the true low energy configuration of a continuous thin film, which can differ from the orientation obtained in conventional epitaxy.

20. DISTRIBUTION/AVAILABILITY OF ABSTRACT UNCLASSIFIED/UNLIMITED ☒ SAME AS RPT ☐ OTIC USERS ☐	21. ABSTRACT SECURITY CLASSIFICATION Unclass
22a. NAME OF RESPONSIBLE INDIVIDUAL<br~~Carl V. Thompson~~ Pamrenke	22b. TELEPHONE NUMBER (Include Area Code)<br~~617/253-7659~~ 202-767-4931
	22c. OFFICE SYMBOL NE

DD FORM 1473, 83 APR EDITION OF 1 JAN 73 IS OBSOLETE.

SECURITY CLASSIFICATION OF THIS PAC

Final Report on Grant No.

AFOSR-85-0154

"Post-Nucleation Heteroepitaxy in Poorly Lattice Matched Systems"

Prepared for

UNITED STATES AIR FORCE

AIR FORCE OFFICE OF SCIENTIFIC RESEARCH

for the period

16 October 1988 to 15 October 1991

Carl V. Thompson
Principal Investigator
Associate Professor of
Electronic Materials
Dept. of Materials Science
and Engineering
MIT, Room 13-5069
Cambridge, MA 02139
(617) 253-7652

TABLE OF CONTENTS

SUMMARY

We have investigated the evolution of thin film structures in the earlier stages of film growth. We have also investigated epitaxial grain growth as a new method for obtaining epitaxial films in poorly lattice-matched systems. We have shown that the As_4 to Ga flux ratio can greatly affect the growth morphology of epitaxial GaAs islands on silicon, and that lower than conventionally used ratios can lead to initial layers and thicker films with greatly improved electronic properties. We have also demonstrated that grain growth in polycrystalline films on single crystal substrates can lead to very thin epitaxial films of higher quality than can be obtained by other techniques. We have also shown that epitaxial grain growth can be used to establish the true low energy configuration of a continuous thin film, which can differ from the orientation obtained in conventional epitaxy.

I. Introduction

This grant was initiated in 1985, with the initial focus on graphoepitaxy, the use of artificial surface topography to align crystalline overlayers. During the period 1985 to 1988, we focused on grain growth in thin films on flat amorphous substrates, and amorphous substrates with artificial surface topography. We ultimately focused on mechanisms for grain growth enhancement, e.g., the use of ion bombardment on metals and semiconductors, and electronically active dopants in semiconductors. While we found that artificial surface topography affects surface-energy-driven secondary grain growth in thin films on amorphous substrates, we were not able to obtain high-quality, fully-oriented films. However, our work on grain growth led us to recognize that grain growth on single crystal substrates could, in principal, lead to high-quality films, as could other post-nucleation microstructural evolution phenomena. After discussions with our AFOSR monitor, in 1988 we changed the title, thrust, and personnel of our program to focus on these post-nucleation processes. Our earlier work has been discussed in detail in earlier annual reports and in the publications given in Section VII. This final report will focus on our work since 1988. It should be noted that new funding for this program was last given in 1988. We have operated on residual funds and other support (e.g., AT&T fellowship support) since October 15, 1989.

We have investigated post-nucleation epitaxial processes involving a variety of mechanisms and a variety of materials. Our interest was originally focused exclusively on epitaxial grain growth. In epitaxial grain growth, a polycrystalline film is deposited on a single crystal substrate, which is then heated. Within the as-deposited polycrystalline film there is a population of grains which are epitaxially aligned. Annealing leads to grain growth during which the epitaxially aligned grains grow while misaligned grains shrink and disappear. Grain growth is therefore a competitive coarsening processes in which epitaxially aligned grains are favored because of their lower energy. Epitaxial alignment through competitive coarsening can also occur in discontinuous films. The theory for this class of processes was developed and presented in reference 1.

Our initial goal was to study epitaxial coarsening in continuous and discontinuous films, in order to test, and as needed, modify the analysis in reference 1. Our ultimate goal was to determine if new epitaxial processes based on epitaxial coarsening in general, and epitaxial grain growth specifically, can provide alternative means of producing high quality epitaxial films in poorly-lattice matched systems. We investigated:

(1) Coarsening in discontinuous metallic films;

(2) The effect of island growth conditions on GaAs-on-Si film quality;

(3) Epitaxial grain growth in CaF-on-Si; and

(4) Epitaxial grain growth in metallic films.

Metals were studied in the first and last cases since they provided experimentally convenient and well-characterized model systems. In our experiments on GaAs-on-Si, much of our initial effort was focussed on obtaining stochiometric polycrystalline GaAs films on Si (as opposed to epitaxial or amorphous films). During these experiments we discovered that the As_4 to Ga flux ratio had a profound effect on the growth morphology of GaAs islands, and ultimately on the electronic quality of the thicker films. Because of the importance of this observation, we also carried out research on this phenomenon. In the following sections, results on each of the four topics listed above will be briefly reviewed.

II. Coarsening in Discontinuous Films

We investigated coarsening of Au islands on amorphous SiO_2 substrates in order to test the analysis described in reference 1 in a simple nonepitaxial experimental system. In discontinuous films, islands coarsen through exchange of material via diffusion on the substrate surface. In our experiments on Au on SiO_2 we were able to demonstrate that the analysis given in reference 1 correctly described the coarsening processes, and could be used to identify the rate limiting kinetic steps. These results are described in Yachin Liu's Ph.D. thesis [reference 2], but have not yet been published.

III. The Effect of Island Growth Conditions on GaAs-on-Si Film Quality

In the course of our attempts to control the initial as-deposited structures of very thin GaAs films deposited via molecular beam epitaxy on Si, we discovered that the As_4 to Ga flux ratio has a profound effect on the morphology of GaAs islands before they coalesce to form a continuous film. Our results are summarized in reference 3, which is also included as Appendix I. When the As_4 to Ga flux ratio was lower than is conventionally used, the islands were significantly larger in the plane of the film than they were thick. Under these conditions, the islands coalesced earlier, to form thinner, smoother continuous films. More importantly, when they were subsequently annealed, they had much lower defect densities than films deposited under conventional conditions. Thicker films grown on these initial layers also had significantly improved electronic properties (see Appendix I). After making this discovery, we went on to further characterize the effect of As_4 to Ga flux ratios on GaAs island growth and to develop a kinetic model which explained our experimental observations. These are described in detail in Joyce Palmer's Ph.D. thesis (reference 4).

IV. Epitaxial Grain Growth in CaF-on-Si

In collaboration with Julia Phillips of AT&T Bell Laboratories, Joyce Palmer also investigated epitaxial grain growth during post-deposition annealing of CaF films on Si. This work was exploratory and was terminated when the CaF-on-Si program was terminated at Bell. The results are described in reference 5 and in more detail in reference 4.

V. Epitaxial Grain Growth in Metallic Films

Much more detailed experiments on epitaxial grain growth have been carried out using metallic films. Metallic systems were used because grain boundary atomic mobilities are relatively high in metals, allowing experimentation at lower temperatures. We initially grew films of Au or Ag on mica and a variety of alkali-halide substrates, especially NaCl. Films were deposited at low temperatures and then annealed *in situ*. Films were subsequently analyzed using thin film x-ray texture goniometry and transmission electron microscopy.

The as-deposited films generally had restricted textures (most grains had specific planes parallel to the plane of the film), with subpopulations of grains also having epitaxial in-plane alignments as well as subpopulations of grains with random in-plane orientations. Annealing was shown to lead to the preferred growth of epitaxially aligned grains, and eventually to films composed entirely of epitaxially aligned material. Through these studies we were able to demonstrate the existence of epitaxial grain growth, and we also showed that epitaxial grain growth can be used to obtain very thin epitaxial films of higher quality than can be obtained by conventional techniques. These experiments are described in reference 6, which is also included as Appendix II.

Experiments on epitaxial grain growth provide a way to determine which crystallographic orientations are truly energy minimizing in continuous thin films. When epitaxial orientations are fixed at the nucleation stage, films have completely different morphologies than the flat continuous films they eventually become. We have observed that the orientations obtained as a result of epitaxial grain growth are not always the same as those obtained during conventional epitaxial growth [see reference 7]. This implies that, at least in these cases, *the orientations obtained via conventional epitaxy are metastable.* We have gone on to further investigate this issue in metal-metal systems. We have especially focused on Ag/Ni films for which there are detailed calculations of the structure and energy of the Ag/Ni interface, as a function of the crystallographic orientations of the Ag and Ni. There are also experimental results for this system not only for conventional epitaxy, but also for rotating sphere experiments (Gao, Dregia, and

Shewmon, Acta Metallurgica 37, p. 1627, 1898). The results from these studies will be summarized in reference 8.

VI. References

1. Thompson, C.V., *Coarsening of Particles on a Planar Substrate: Interface Energy Anistropy and Application to Grain Growth in Thin Films,* Acta Metallurgica 36, 1988.

2. Liu, Y., *Coplanar-Spherical-Particle Coarsening in Discontinuous Ultrathin Polycrystalline Gold Films on Amorphous Silicon-Nitride Substrates,* Ph.D., Thesis, Department of Materials Science and Engineering, MIT, Cambridge, MA, February 1991.

3. Palmer, J.E., Burns, G., Fonstad, C.G., and Thompson, C.V., *The Effect of As_4 Overpressure on Initial Growth of Gallium Arsenide on Silicon by MBE,* Appl. Phys. Letts. 55, 1989.

4. Palmer, J.E., *Evolution of Microstructure in Ultra-Thin Films of GaAs and CaF_2 on Single Crystal Silicon,* Ph.D. Thesis, Department and Electrical Engineering and Computer Science, MIT, Cambridge, MA, May 1989.

5. Phillips, J.M., Palmer, J.E., Hecker, N.E., and Thompson, C.V., *The Effect of Annealing on the Structure of Epitaxial CaF_2 Films on Si(100),* MRS Symposium Proceedings 148, 1989.

6. Thompson, C.V., Floro, J., and Smith, H.I., *Epitaxial Grain Growth in Thin Metal Films,* J. Appl. Phys. 67 (9), May 1990.

7. Floro, J.A. and Thompson, C.V., *Epitaxial Grain Growth and Orientation Metastability in Heteroepitaxial Thin Films,* Materials Research Society Symposium Proceedings 187, 1991.

8. Floro, J.A., *Epitaxial Grain Growth,* Ph.D. Thesis, Dept. of Materials Science and Engineering, MIT, Cambridge, MA, expected completion June 1992.

VII. Publications

October 16, 1988 to October 15, 1991: Same as above.

Prior to October 16, 1988:

Atwater, H.A., Thompson, C.V., and Smith, H.I., *Interface Limited Grain Boundary Motion During Ion Bombardment,* Phys. Rev. Lett. 60, 1988.

Atwater, H.A., Thompson, C.V., and Smith, H.I., *Ion Bombardment Enhanced Grain Growth in Germanium, Silicon, and Gold Thin Films,* J. Appl. Phys. 64, 1988.

Atwater, H.A., Smith, H.I., and Thompson, C.V., *Enhancement of Grain Growth in Ultra Thin Germanium Films by Ion Bombardment*, Mat. Res. Soc. Symp. Proc. 51, 1986, eds. H. Kurz, G.L. Olson, J.M. Poate, Materials Research Society.

Atwater, H.A., Smith, H.I., and Thompson, C.V., *Ion Beam Enhanced Grain Growth in Thin Films*, Beam-Solid Interactions and Transient Processes Symposium, Materials Research Society Meetings, Dec. 1986, Mat. Res. Soc. Symp. Proc. 74, 1987.

Atwater, H.A., Thompson, C.V., and Smith, H.I., *Transition State Model for Grain Boundary Motion During Ion Bombardment* (Invited), Proceedings of the Fall 1987 Materials Research Society Symposium on the Fundamentals of Beam-Solid Interactions and Transient Thermal Processing, Boston, MA.

Atwater, H.A., *Ion Beam Enhanced Grain Growth in Thin Films*, Ph.D. Thesis, Department of Electrical Engineering and Computer Science, Massachusetts Institute of Technology, June 1987.

Cammarata, R.C., Thompson, C.V., and Garrison, S.M., *Secondary Grain Growth During Rapid Thermal Annealing of Doped Polysilicon Films*, presented at Spring MRS Meeting, 1987, Mat. Res. Soc. Symp. Proc. 92, 1987.

Garrison, S.M., Cammarata, R.C., Thompson, C.V., and Smith, H.I., *Surface-Energy-Driven Grain Growth During Rapid Thermal Annealing (<10s) of Thin Silicon Films*, J. Appl. Phys. 61, 1987.

Garrison, S.M., *The Kinetics of Secondary Grain Growth in Rapidly Thermal Annealed Thin Silicon Films*, S.M. Thesis, Department of Materials Science and Engineering, Massachusetts Institute of Technology, Cambridge, MA, June 1986.

Kim, H.-J. and Thompson, C.V., *Compensation of Grain Growth EDnhancement in Doped Silicon Films*, Appl. Phys. Lett. 48, 1986.

Kim, H.-J. and Thompson, C.V., *The Effect of Dopants on Grain Boundary Mobility in Silicon*, 4th International Symposium on Grain Boundary Structure and Related Phenomena, Japan Institute of Metals, Supplement to Trans. of Jap. Inst. of Metals 27, 1986.

Kim, H.-J. and Thompson, C.V., *The Effects of Dopants on Surface-Energy-Driven Grain Growth in Ultrathin Si Films*, Proceedings of the Fall Meeting of the Materials Research Society, Boston, MA. Dec. 2-6, 1985, Mat. Res. Soc. Symp. Proc. 54, 1986.

Palmer, J., Thompson, C.V., and Smith, H.I., *Grain Growth and Grain Size Distribution in Thin Germanium Films on SiO_2*, J. Appl. Phys. 62, 1987.

Palmer, J.E., *Secondary Grain Growth in Ultra Thin Germanium Films on Silicon Dioxide*, M.S. Thesis, Department of Electrical Engineering and Computer Science, Massachusetts Institute of Technology, Cambridge, MA, August 1985.

Smith, H.I., Geis, M.W., Thompson, C.V., and Chen, C.K., *Crystalline Films on Amorphous Substrates by Zone Melting and Surface-Energy-Driven Grain Growth in Conjunction with Patterning*, Mat. Res. Soc. Symp. Proc. 53, 1986, eds. A. Chiang, M.W. Geis, L. Pfeiffer, Materials Research Society.

Thompson, C.V., *Secondary Grain Growth in Thin Films of Semiconductors: Theoretical Aspects*, J. Appl. Phys. 58, 1985.

Thompson, C.V., *Coarsening of particles on a Planar Substrate: Interface Energy Anisotropy and Application to Grain Growth in Thin Films*, Acta Metallurgica 36, 1988.

Thompson, C.V. and Smith, H.I., *Secondary Grain Growth in Thin Films, Phase Transitions in Condensed Systems - Experiment and Theory,* Mat. Res. Soc. Symp. Proc. 57, 1987, eds. G.S. Cargill III, F. Spaepen, K.N. Tu, Materials Research Society.

Thompson, C.V., *Dopant and Ion Beam Enhanced Grain Growth in Polycrystalline Silicon Films* (Invited), in Diffusion Processes in High Technology Materials, ed. by D. Gupta and A.D. Romig, Jr., Symposium of TMS/AIME fall meeting, Cincinnati, OH, 1987.

Thompson, C.V., *Grain Growth in Polycrystalline Silicon Films* (Invited), Proceedings of the Fall 1987 Materials Research Society Symposium on Polysilicon Films and Interfaces, Boston, MA.

Thompson, C.V., *Observations of Grain Growth in Thin Films* (Invited), Proceedings of the Topical Symposium on Microstructural Science for Thin Film Metallization in Electronic Applications, Spring Meeting of the Metallurgical Society of the American Institute of Mining, Metallurgical, and Petroleum Engineers, Phoenix, AZ, Jan. 1988.

Wong, C.C., Smith, H.I., and Thompson, C.V., *Surface-Energy-Driven Secondary Grain Growth in Thin Au Films,* Appl. Phys. Lett. 48, 1986.

Wong, C.C., Smith, H.I., and Thompson, C.V., *Room Temperature Grain Growth in Thin Au Films, 4th International Symposium on Grain Boundary Structure and Related Phenomena,* Supplement to Trans. of Jap. Inst. of Metals 27, 1986.

Wong, C.C., Smith, H.I., and Thompson, C.V., *Secondary Grain Growth and Graphoepitaxy in Thin Au Films on Submicrometer-Period Gratings,* Mat. Res. Soc. Symp. Proc. 47, 1985, Materials Research Society.

Wong, C.C., Secondary Grain Growth and Graphoepitaxy in Thin Au Films, Ph.D. Thesis, Department of Materials Science and Engineering, Massachusetts Institute of Technology, Cambridge, MA, February 1986.

APPENDIX I

EFFECT OF As_4 OVERPRESSURE ON INITIAL GROWTH OF CALLIUM ARSENIDE ON SILICON BY MBE

Reprinted from Applied Physics Letters 55, 1989.

Effect of As_4 overpressure on initial growth of gallium arsenide on silicon by molecular beam epitaxy

J. E. Palmer, G. Burns, and C. G. Fonstad
Department of Electrical Engineering and Computer Science, Massachusetts Institute of Technology, Cambridge, Massachusetts 02139

C. V. Thompson
Department of Materials Science and Engineering, Massachusetts Institute of Technology, Cambridge, Massachusetts 02139

(Received 10 April 1989; accepted for publication 5 July 1989)

We have demonstrated great improvement in the smoothness and defect density of GaAs films on Si by lowering the arsenic overpressure during growth of the initial layer (the first 500 Å) of GaAs. We have studied the morphology and defect density of GaAs on Si films in which the initial layers were grown under either low As_4 overpressure ($7As_4$:1Ga, beam equivalent pressure) or high As_4 overpressure ($15As_4$:1Ga) conditions, with a constant gallium flux. In the early stages of growth there is a significant change in island morphology depending on the As_4 overpressure. There is dramatic improvement of surface smoothness and crystal quality with reduced arsenic overpressure for 500-Å-thick layers both immediately after growth at 350 °C and after heating to 580 °C. Diodes fabricated in 3.5-μm-thick films grown on initial layers that were grown under low arsenic overpressure have a very sharp reverse breakdown at voltages as high as 45 V, whereas diodes fabricated in films grown on initial layers that were grown under high arsenic overpressure have a soft reverse breakdown at about 5 V. This demonstrates a significant reduction in the density of electrically active defects in the thick GaAs films with decreasing arsenic overpressure conditions during growth of the initial 500 Å of GaAs on Si. The improvement in film quality for low As_4 overpressures is discussed in terms of the observed changes in island morphology.

Heteroepitaxy of GaAs on Si is of interest for monolithic integration of optoelectronic GaAs devices with well-established Si technology. Most, if not all molecular beam epitaxy (MBE) GaAs on Si is grown using a two-step process,[1] in which a thin (200–1000 Å) GaAs film is first deposited at a relatively low temperature (300–400 °C) and at a slow rate (1000–2000 Å/h),[2] followed by growth of thick layers at higher temperatures (~580 °C) and higher rates (~1 μm/h). It has been shown that GaAs forms islands on Si,[3] and that in the lower temperature range, the islands are small and closely spaced so that a continuous film is formed within a few hundred angstroms of growth.[4] Recently, Chand *et al.* reported improved Schottky diode performance using a $10As_4$:1Ga beam equivalent pressure ratio during initial layer growth, approximately half that used during device layer growth.[5] We have used reflection high-energy electron diffraction (RHEED), scanning electron microscopy (SEM), as well as plan-view and cross-sectional transmission electron microscopy (TEM) to study the effect of As_4 overpressure on the morphology and crystal quality of GaAs islands and 500-Å-thick initial layers of GaAs on Si. In order to relate the quality of the initial layer to electrical properties, we have made diodes in thick films grown on the various initial layers.

n-type (10^{16}/cm^3, arsenic-doped) Si wafers cut 4° off (100) toward [011] were chemically cleaned with a solution of $5H_2O$:$1H_2O_2$:$1NH_4OH$ to remove organic contaminants. This treatment also produces a very thin SiO_2 layer, which was removed using a $1HF$:$1H_2O$ solution. The wafers were oxidized ($5H_2O$:$1H_2O_2$:1HCl) and etched ($1HF$:$1H_2O$) three times before the final oxide was grown using a $1H_2O$:$1H_2O_2$:3HCl solution. The wafers were immediately mounted on molybdenum blocks with indium, and loaded into a Riber MBE system. The oxide layer was removed by heating *in situ* to 850 °C for 15 min. The substrate was exposed to the As_4 after the substrate had cooled to 400 °C. RHEED showed a 2×4 reconstruction. Growth was initiated when the substrate temperature reached 350 °C. Four sets of samples were grown for this study.

Set A. 30 Å of GaAs was deposited at a rate of 2000 Å/h at 350 °C, under both low As_4 overpressure ($7As_4$:1Ga, beam equivalent pressure) and high As_4 overpressure ($15As_4$:1Ga), and the samples were removed from the MBE system.

Set B. 500-Å-thick initial layers were grown at a rate of 2000 Å/h at 350 °C under both low As_4 overpressure and high As_4 overpressure and were removed from the system.

Set C. The growth for set B was repeated, then the substrates were brought to 580 °C under high As_4 overpressure, and removed from the system.

Set D. The growth for set C was repeated, followed by growth of a 0.5-μm-thick heavily doped layer (10^{18}/cm^3 Si) and a 2.5-μm-thick layer (10^{16}/cm^3 Si) and a 0.5-μm-thick heavily doped layer (10^{18}/cm^3 beryllium) at a rate of 1 μm/h under high As_4 overpressure.

As samples were examined *in situ* using RHEED, and samples from sets A, B, and C were examined by SEM, plan-view, and cross-sectional TEM. Diodes were fabricated in the samples from set D and their current-voltage (*I-V*) characteristics were studied.

Figures 1 and 2 are SEM and cross-sectional TEM (XTEM) micrographs, respectively, of the nominally 30-Å-

 0003-6951/89/360990-03$01.00

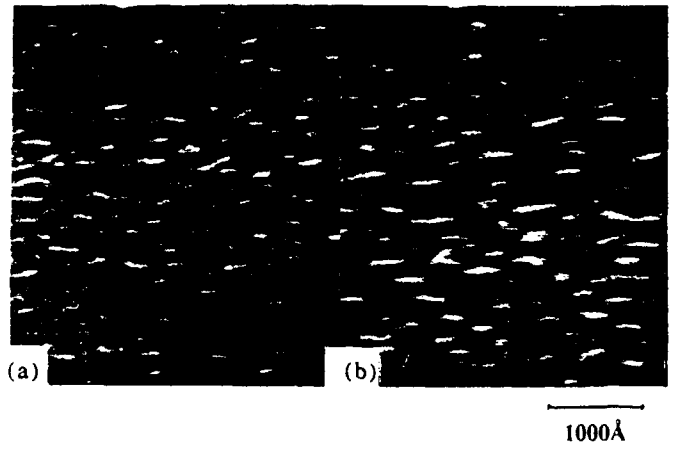

FIG. 1. SEM micrographs of nominally 30-Å-thick films (sample set A) grown on Si at 350 °C under (a) low arsenic overpressure ($7As_4$:1Ga, beam equivalent pressure) and (b) high arsenic overpressure (15:1).

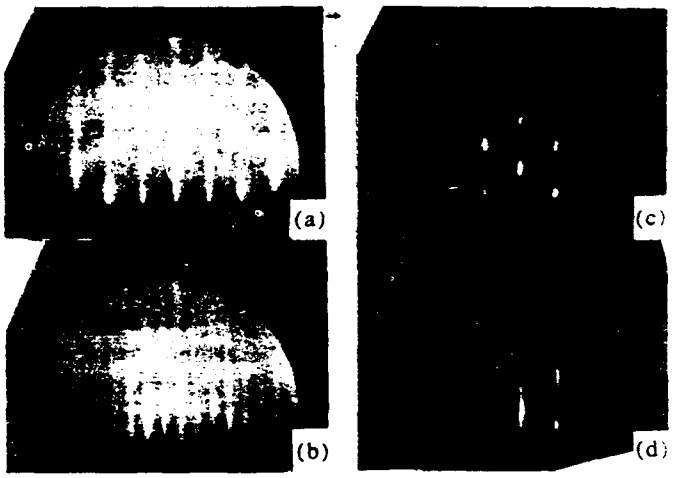

FIG. 3. RHEED patterns of 500-Å-thick GaAs films as-grown at 350 °C [(a) and (c)] and heated to 580 °C [(b) and (d)]. (sample sets B and C.) [(a) and (b)] were grown at $7As_4$:Ga, [(c) and (d)] at $15As_4$:1Ga.

thick samples grown under both low and high As_4 overpressures (set A). The SEM photos show that there is a significant increase (about a factor of 2) in the island density under low As_4 overpressure. The XTEM micrographs reveal that the islands formed under low As_4 overpressure are flatter than those grown under high As_4 overpressure. The difference is also noticeable in the RHEED patterns photographed immediately after growth.

The direct implications of this result are that initial layers grown under low As_4 overpressure become continuous earlier (i.e., at smaller thicknesses) than layers grown under high As_4 overpressure, and that in the early stages of growth, films of the same thickness are smoother when grown under low As_4 overpressure. Using a Johnson–Mehl–Avrami[6] analysis, the thickness at which a film becomes continuous can be approximated by[7]

$$t = \frac{h}{r}\left(\frac{-\ln(1-x)}{I_0\pi}\right)^{1/2} = 2A\left(\frac{-\ln(1-x)}{I_0\pi}\right)^{1/2}, \quad (1)$$

where t is the film thickness, h is the average island height and r is the average island radius, x is fraction of the surface covered by islands, I_0 is the island density in number per unit area, and $A = h/2r$ is the aspect ratio of the islands. From Fig. 2 we estimate that the aspect ratios for islands grown under high and low As_4 overpressure are 0.5 and 0.1, respectively. From plan-view micrographs (not shown here), we have measured the island density under high As_4 overpressure to be $4\times10^{10}/cm^2$, and we infer from Fig. 1 that the island density under low As_4 overpressure is twice that number, $8\times10^{10}/cm^2$. Measurements could not be made directly in the low As_4 overpressure case because island coalescence had already begun at the nominal thickness of 30 Å. Using Eq. (1), with $x = 0.95$, the films will become continuous at 70 and 490 Å, respectively.

Figure 3 shows RHEED patterns for the 500-Å-thick initial layers as-grown (set B) and after heating to 580 °C (set C). In both cases, the films grown under low As_4 overpressure are smoother than those grown under high As_4 overpressure. The RHEED pattern of the low As_4 overpres-

FIG. 2. Cross-sectional TEM micrographs of nominally 30-Å-thick films (sample set A) grown on Si at 350 °C under (a) low arsenic overpressure ($7As_4$:1Ga, beam equivalent pressure) and (b) high arsenic overpressure (15:1).

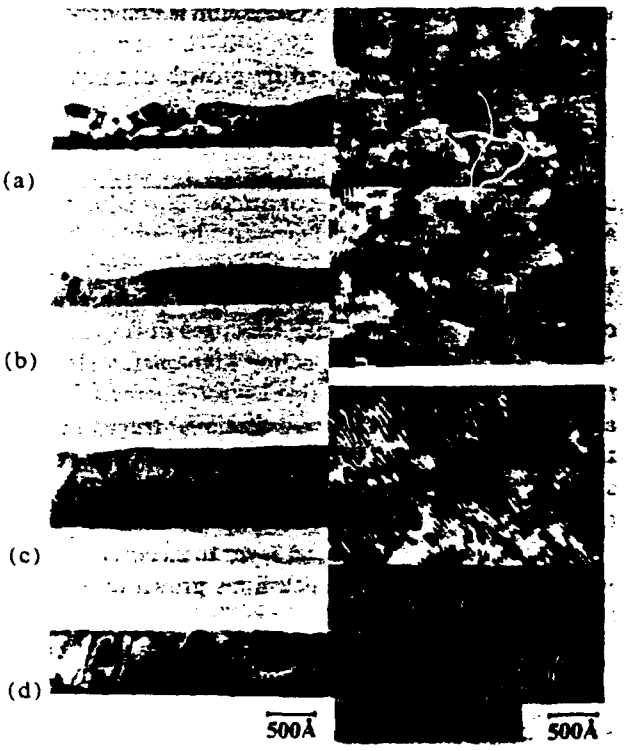

FIG. 4. Plan-view and cross-sectional TEM micrographs of 500-Å-thick GaAs films as-grown at 350 °C [(a) and (c)] and heated to 580 °C [(b and (d)]. (sample sets B and C.) [(a) and (b)] were grown at $15As_4$:1Ga [(c) and(d)] at $7As_4$:1Ga.

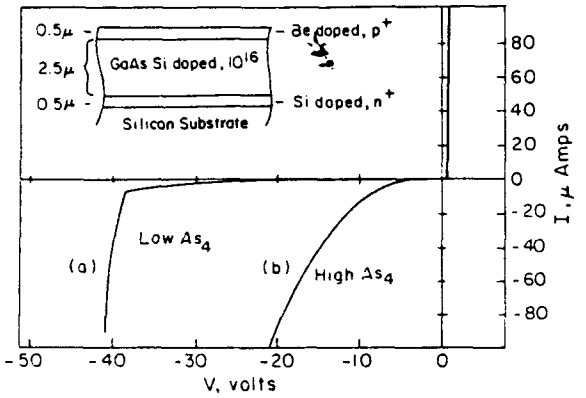

FIG. 5. *I-V* characteristics for *p-n* diodes fabricated in films grown on initial layers that were grown under low As_4 overpressure (a) have a sharp avalanche reverse breakdown at ~ 37 V, whereas the diodes fabricated in films grown on initial layers that were grown under high As_4 overpressure (b) have a soft reverse breakdown at about 5 V.

sure film brought to 580 °C is, in fact, indistinguishable from a flat bulk GaAs (100) surface. Figure 4 shows the plan-view and cross-sectional TEM micrographs of the 500 Å films (sets B and C). Note that *both* the initial and final density of twins and stacking faults are dramatically reduced in low As_4 overpressure films. The moiré fringes seen in the plan-view micrographs indicate both superior crystal quality and a surface smoothness in low As_4 overpressure films.

Figure 5 shows the *I-V* characteristics of diodes fabricated in 3.5-μm-thick films grown under high As_4 overpressure on initial layers grown under high and low As_4 overpressures (set D). The most striking difference is in the reverse characteristics, which show a sharp breakdown at ~ 37 V for the film grown on a low As_4 overpressure initial layer. Breakdown voltages as high as 45 V were observed. The GaAs film is depleted all the way through the lightly doped region to the n^+ region. In contrast, diodes fabricated in thick films grown on initial layers that were grown under high arsenic overpressure have a soft reverse breakdown near 5 V. This indicates that the number of crystalline defects that act as generation and recombination sites is dramatically reduced in the films grown on the initial layers that were grown under low As_4 overpressure. These results are consistent with those of Chand *et al.*[5]

We assert that the low As_4 overpressure films had fewer defects from the start because of the flatter morphology of the growing islands. The relationship between island morphology and defect incorporation is not clear, but is thought to be related to the occurrence of growth errors on (111) facets[8] and/or the incorporation of misfit dislocations during initial growth.[9] Twins and stacking faults in the initial layer, which are the result of growth errors on (111) facets, are thought to be sources for defects that "thread" into the film (commonly called threading dislocations). Flatter islands, since they have less exposed (111) facet area on which growth errors occur, will have fewer twins and stacking faults, and therefore the subsequently grown layer will have fewer defects. This is true in spite of the fact that the island density is higher at low arsenic overpressures. Alternatively, the reduction in defect density could be due to a change in the mechanism by which misfit dislocations are generated and incorporated at the interface. At low As_4 overpressure, the film is thinner when it becomes continuous. It is likely that not all of the lattice mismatch has been accommodated. The misfit will be accommodated by the introduction of defects in a continuous film. In contrast, films that coalesce at larger thicknesses will already have developed defects in the individual islands to accommodate the lattice mismatch. The exact mechanism of defect incorporation to accommodate lattice mismatch need not be the same for islands and continous films. It is possible that misfit dislocations are generated in a way that results in fewer bulk defects in a continuous film than in single islands.

We have developed a growth model for GaAs islands on Si based on a longer period of mobility for Ga adatoms under low As_4 overpressure.[10] This model predicts that when Ga adatoms have a longer period of mobility on the surface, the number of nuclei will increase and the radial growth rate of the islands is enhanced during the initial stages of island formation, consistent with the experimental observations reported here.

We have demonstrated that the As_4 overpressure during initial layer growth of GaAs on Si affects the morphology of the GaAs islands, the density of twins and stacking faults in the initial layers, and the number of electrically active defects in subsequent device layers. GaAs islands are flatter when grown under low As_4 overpressure, and the island density is somewhat higher. Films grown under low As_4 overpressure probably have fewer twins and stacking faults and have smoother surfaces, because of the difference in island morphology in the early stages of growth. The excellent quality of the device layers has been demonstrated with diodes in which the entire 2.5-μm-thick layer can be depleted without soft breakdown.

This work was sponsored by the Air Force Office of Scientific Research (AFOSR-85-0154) and the National Science Foundation (ECS-88-07498). G. Burns is an IBM resident. The authors would like to thank Dr. Tow C. Chong of the National University of Singapore who initiated this work while he was at MIT, and Dr. Wolfgang Stoltz of the Max–Planck Institut for helpful discussions.

[1] Mater. Res. Soc. Symp. Proc. **67** (1986), **94** (1987), and **116** (1988), and references therein.
[2] This initial layer is sometimes called the nucleation layer or buffer layer, but since "buffer layer" can also refer to thick layers grown under homoepitaxial conditions, and since both nucleation and growth occur in this first GaAs layer, we will refer to it as the initial layer.
[3] S. J. Rosner, S. M. Kock, S. Laderman, and J. H. Harris, Mater. Res. Soc. Symp. Proc. 67, 77 (1986).
[4] D. K. Biegelson, F. A. Ponce, J. C. Tramontana, and R. D. Yingling, Appl. Phys. Lett. 52, 1779 (1986).
[5] N. Chand, J. P. van der Ziel, J. S. Weiner, A. M. Sergent, and D. V. Lang, Mater. Res. Soc. Symp. Proc. (Fall 1988).
[6] J. W. Christian, *The Theory of Transformations in Metals and Alloys, Part I*, 2nd ed. (Pergamon, New York, 1975), p. 15.
[7] Equation 1 was obtained by assuming that (i) the islands are disk shaped with fixed aspect ratio, (ii) the number of islands does not change with time, and (iii) the thickness at which the film becomes continuous is given by the island height when the islands cover a large fraction x of the surface. x is related to the radius of the islands by $-\ln(1-x) = I_0\pi r^2$.
[8] F. Ernst and P. Pirouz, J. Appl. Phys. 64, 4526 (1988).
[9] J. Y. Tsao and B. W. Dodson, Appl. Phys. Lett. 53, 848 (1988).
[10] J. E. Palmer, C. V. Thompson, G. B. Burns, and C. G. Fonstad (unpublished research); J. E. Palmer, Ph.D. thesis, Department of Electrical Engineering and Comptuter Science, Massachusetts Institute of Technology, Cambridge, MA, 1989.

APPENDIX II

EPITAXIAL GRAIN GROWTH IN THIN METAL FILMS

Reprinted from Journal of Applied Physics 67 (9), May 1990.

Epitaxial grain growth in thin metal films

C. V. Thompson and J. Floro
Department of Materials Science and Engineering, Massachusetts Institute of Technology, Cambridge, Massachusetts 02139

Henry I. Smith
Department of Electrical Engineering and Computer Science, Massachusetts Institute of Technology, Cambridge, Massachusetts 02139

(Received 13 October 1989; accepted for publication 10 January 1990)

Epitaxial alignment has been obtained by means of grain growth in polycrystalline films deposited on single-crystal substrates. A theory for epitaxial grain growth is outlined and results given for experiments on Au, Al, Cu, and Ag films on vacuum-cleaved NaCl, KBr, KCl, or mica. Epitaxial grain growth provides a fundamentally different alternative to conventional epitaxy, and can lead to very thin films with improved continuity and crystalline perfection, as well as non-lattice-matched orientations.

I. INTRODUCTION

When strong chemical interactions exist between a film and a substrate, and the lattice mismatch is less than about 4%,[1] films can grow epitaxially via the Frank–van der Merwe mechanism,[2] in which the film surface propagates by atom-by-atom attachment, often resulting in layer-by-layer growth. In this case, adatoms coalesce to form ledges or attach to preexisting ledge sites, and epitaxial growth results naturally as a pseudomorphic extension of the substrate lattice. However, in the vast majority of film-substrate combinations, chemical interactions and lattice mismatches are such that the film instead grows by three-dimensional nucleation of islands, which then grow until they impinge on other islands and coalesce to form a film. This mode of growth is often referred to as Volmer–Weber growth.[3]

Epitaxial films can result from Volmer–Weber growth in two fundamentally different ways:

(i) Nuclei can be uniformly epitaxially oriented, so that the resulting islands coalesce to form a single-crystal film [see Fig. 1(a)] or

(ii) Epitaxial alignment may result from *post-nucleation* processes.

The first mechanism is usually referred to as *Volmer–Weber epitaxy*.[3]

In most deposition processes, critical nuclei are composed of at most a few atoms.[4] In this case, it is likely that in Volmer–Weber systems, nuclei will not have well-defined or uniform crystallographic orientation relationships with their substrates, and the second category of epitaxial mechanisms listed above will apply. Post-nucleation epitaxial alignment in Volmer–Weber systems can in principal occur by island rotation[5] or coarsening of isolated islands through exchange of material via substrate surface diffusion.[6] It can also occur via grain-boundary motion during and after island coalesence.

A clear example of the latter mechanism would be a polycrystalline, continuous film that undergoes grain growth, resulting in a single-crystal or near-single-crystal film. This process is illustrated in Fig. 1(b) and will be referred to as *epitaxial grain growth*. While experimental evidence for this mechanism has been previously reported,[7] no detailed demonstration and discussion of epitaxial grain growth exists, despite the fact that epitaxial grain growth can in principal occur in a wide variety of systems. In this paper we will outline the extension of the theory of surface-energy-driven secondary-grain growth in thin films to include the theory of epitaxial grain growth. We will also report experimental results that demonstrate this mechanism in Au, Cu, Al, and Ag films on NaCl, KCl, KBr, and mica.

II. SURFACE-ENERGY-DRIVEN SECONDARY-GRAIN GROWTH IN THIN FILMS

Grain growth occurs in order to reduce the total energy of a solid. In the case of bulk materials, grain growth is driven by the elimination of grain-boundary energy which accompanies the reduction in the total area of grain boundaries per unit volume. Hillert[8] has argued that for individual grains, the rate of growth can be approximated by

$$\dot{r} = \frac{dr}{dt} = M\gamma_{gb}\left(\frac{1}{\bar{r}} - \frac{1}{r}\right), \tag{1}$$

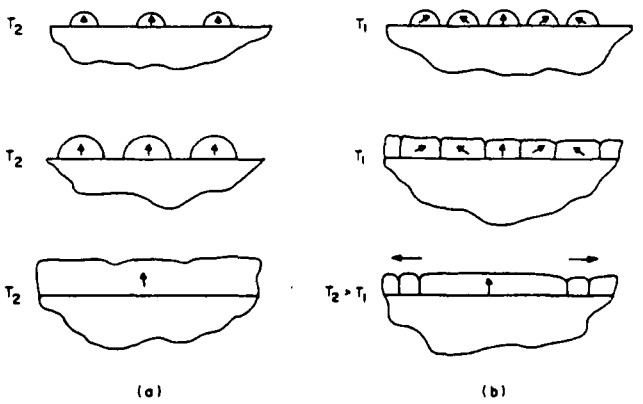

FIG. 1. Schematic cross section views of films grown by (a) conventional Volmer–Weber epitaxy by nucleation, growth, and coalesence of epitaxially oriented islands deposited at elevated temperatures (e.g., T_2), and (b) epitaxial grain growth at a temperature T_2 in a polycrystalline film deposited on a single-crystal substrate at a lower temperature T_1.

 0021-8979/90/094099-06$03.00

where M is the average grain boundary mobility, γ_{gb} is the average grain-boundary energy, $\bar{r}$ is the average grain radius, and r is the radius of the grain under consideration. Hillert also argued that, given Eq. (1),

$$\dot{\bar{r}} = \frac{M}{8}\frac{\gamma_{gb}}{\bar{r}}. \tag{2}$$

An expression of this form can also be derived in other ways[9,10] and is generally believed to adequately fit experimental results in pure materials.

As in bulk materials, grain growth in thin films also occurs in order to minimize the total energy of the film. However, when the grain size is comparable to or larger than the film thickness, the energy of a grain in a thin film includes not only the energy associated with the grain boundaries, but also the energy of the top and bottom surfaces of the film. In this case, for a free-standing thin film or a film bounded by identical surfaces, Thompson[6,10] has argued that the thin-film analog of Eq. (1) is

$$\dot{r} = M\left[\frac{2(\gamma_s^* - \gamma_s)}{h} + \gamma_{gb}\left(\frac{1}{\bar{r}} - \frac{1}{r}\right)\right], \tag{3}$$

where, as illustrated in Fig. 2, h is the film thickness, γ_s is the surface energy of the growing grain and γ_s^* can be taken to be the average surface energy of the film.

If the surface energy γ_s is not a function of the crystallographic orientation of the film, then Eq. (3) reduces to Eq. (1). However, γ_s is in fact usually strongly dependent on the crystallographic orientation of a grain, so that those grains with orientations that lead to low surface energies will grow faster than those grains with other orientations. This leads to preferred growth of a subset of the grains with restricted orientations, as illustrated in Fig. 2(a), so that grain growth in thin films leads to an evolution in the average crystallographic *orientation* of the film, as well as the average grain size.

The preferential growth of a few grains within a larger population of smaller grains is referred to as secondary or abnormal grain growth. In the case described above, in which preferred growth results from surface energy anisotropy, the process is known as surface-energy-driven secondary-grain growth (SEDSGG). Secondary grains that grow abnormally fast will continue to grow until they impinge on grains with similar surface energies. In free-standing films or films sandwiched between amorphous materials, SEDSGG should result in films composed of large grains with monomodally distributed sizes and with restricted or uniform fiber texture, i.e., all grains having the same planes parallel to the plane of the film, but random in-plane orientations. This has been confirmed experimentally.[11-13]

In thin films, normal grain growth is often restricted by "the specimen thickness effect,"[12,14] whereby stagnation of grain growth occurs when $\bar{r}$ is approximately equal to twice the film thickness.[12] In this case, subsequent grain growth involves the *exclusive* growth of grains with orientations that minimize γ_s, while all other grains neither grow nor shrink. Therefore, the secondary grains grow into a static matrix for which $\bar{r} \cong 2h$. When the secondary grains are large (i.e., $r_s \gg \bar{r}$) but have not yet impinged, Eq. (3) for secondary grains reduces to

$$\dot{r}_s \cong M\left(\frac{2(\gamma_s^* - \gamma_s) + \gamma_{gb}}{h}\right), \tag{4}$$

where γ^* now is the average surface energy of the normal grains. From this result it can be readily seen that the rate of secondary-grain growth is expected to be inversely proportional to the film thickness, and, prior to impingement, the secondary-grain size should be proportional to time.

For films that are attached to substrates and have only one free surface, as illustrated in Fig. 2(b), the energy of the free surface of the film, γ_s, and the energy of the film-substrate interface, γ_i, need not be equal. In this case, Eq. (3) should be modified to become

$$\dot{r}_s = M\left[\frac{(\gamma_s^* - \gamma_s)}{h} + \frac{(\gamma_i^* - \gamma_i)}{h} + \gamma_{gb}\left(\frac{1}{\bar{r}} - \frac{1}{r}\right)\right], \tag{5}$$

where, in analogy with γ_s^*, γ_i^* is related to the average *interface* energy of the film. If the substrate is amorphous, it is again expected, and observed,[15] that SEDSGG will lead to films with restricted fiber texture but random in-plane orientations. On the other hand, if the substrate is a single crystal, then γ_i should depend on the *in-plane orientation* of a grain, as well as its fiber texture. Therefore, SEDSGG in films on single-crystal substrates should generally lead to films with three-dimensionally constrained, epitaxial orientations, i.e., epitaxial grain growth (EGG) should occur.

The degree to which orientational selectivity occurs during grain growth depends on many factors, but especially on the detailed nature of the relationship between γ_i and the relative orientations of the substrate and the grains within a film. For example, considering the schematic Wulff[16] plot in Fig. 3(b) which shows γ_i for in-plane rotations θ, the number of orientations for which $\gamma_i < \gamma_i^*$ will be a function of the number and depth of the interface energy minima. Also, the degree to which in-plane orientations will be restricted near

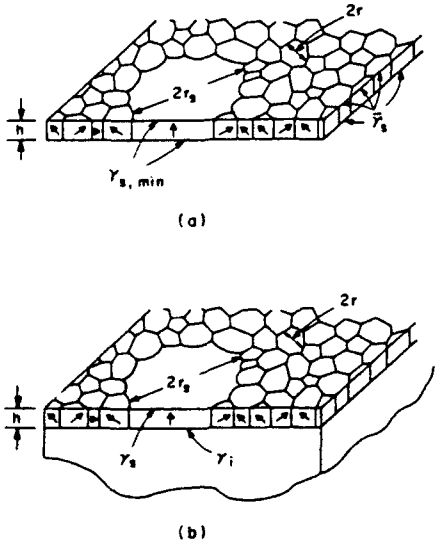

FIG. 2. Schematic illustration of secondary grains in (a) a free-standing film or a film bound by identical materials both on the top and the bottom, and (b) a film on a substrate.

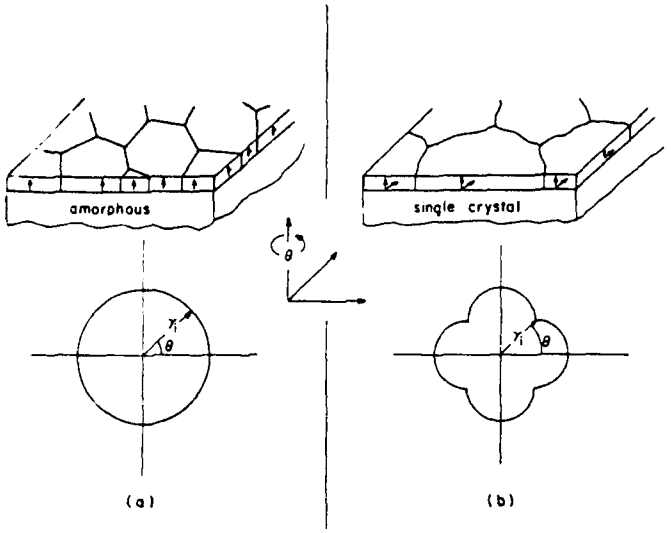

FIG. 3. Sketches showing the results of surface-energy-driven secondary-grain growth on (a) an amorphouse substrate (leading to near-uniform fiber texture but *not* in-plane orientation) and (b) a single-crystal substrate (leading to near-uniform texture *and* in-plane orientation). Also shown are schematic Wulff plots for the interface energy γ_i for grains with a fixed fiber texture but variable in-plane orientation specified by θ.

a γ_i-minimizing orientation will depend on the steepness of the sides of the cusps in the Wulff plot.

It should be noted that during SEDSGG in films on substrates, the *total* energy of the film must be minimized. A given film crystallographic orientation may not lead to minimization of *both* the surface energy and interface energy of the film. Minimization of the total energy of a film may lead to dominance of grains with orientations that minimize neither γ_f nor γ_s, but constitute a compromise that reduces both γ_f and γ_s. Therefore, in EGG, as presumably in other mechanisms of epitaxy, the free surface energy of the film can play an important role in orientation selection. The final orientation resulting from epitaxial grain growth need not be the same orientation that results from other epitaxial processes, such as Volmer–Weber epitaxy, in which energy minimization occurs for crystals with three-dimensional shapes.[17]

III. EXPERIMENTAL METHODS

Films of Au, Ag, Cu, and Al have been deposited on freshly vacuum-cleaved muscovite mica, NaCl, KCl, or KBr. Films were deposited by electron-beam evaporation in a Balzers ultra high-vacuum (UHV) system at a rate of 1–10 Å/s. The pressure in the system prior to deposition was always lower than 1×10^{-9} Torr and never exceeded 2×10^{-8} Torr during deposition, with a combined partial pressure of H_2O and O_2 being less than 5×10^{-10} Torr. Films deposited for studies of epitaxial grain growth were always deposited at room temperature. In some cases, films were deposited at room temperature and then heated and annealed immediately after deposition *without removal from the vacuum system*. Films that were deposited in order to study conventional epitaxy were deposited on substrates held at elevated temperatures.

Substrate preparation is known to have a strong effect on conventional epitaxy in general and on epitaxial growth of metal films on mica and NaCl specifically.[18,19] This was found to be the case for epitaxial grain growth as well. In order to get reproducible results, deposition on vacuum-cleaved substrates was required (as opposed to cleaving outside the vacuum system). It was also necessary that annealing be done under UHV conditions without exposure of the films to atmosphere.

After deposition and vacuum annealing, if such was done, substrates were removed and prepared for transmission electron microscopy by aqueous dissolution of the NaCl, KCl, or KBr or by "tape-thinning"[20] of the mica. Films were then characterized using transmission electron diffraction (TED) as well as bright-field and dark-field transmission electron microscopy (TEM). In order to determine the relative orientation of the film and substrate, it was required that an electron-transparent section of substrate be retained under the film after the thinning process. For Al and Cu on mica, this was straightforward. However, for Au on mica, x-ray pole figures of both the film and substrate were required in order to provide unambiguous determination of relative orientations.

IV. RESULTS

Figure 4 shows TED patterns, bright-field transmission electron micrographs, and dark-field transmission electron

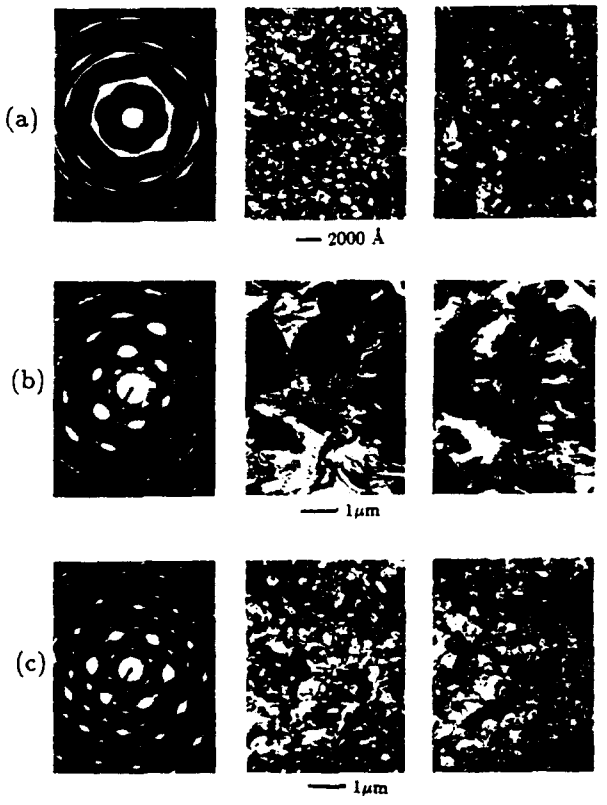

FIG. 4. Transmission electron diffraction patterns (left), bright-field TEM micrographs (center), and dark-field TEM micrographs (right) of 650-Å-thick Au films (a) as-deposited on vacuum-cleaved (001) mica at room temperature, (b) deposited at room temperature and annealed *in situ*, and (c) as deposited directly at 400 °C.

micrographs of 650-Å-thick gold films deposited on a vacuum-cleaved (001) surface of mica. Figure 4(a) shows results for a film as-deposited at room temperature. The grain size is 500–2000 Å. As indicated by the TED pattern, the as-deposited grains have an almost uniform (111) fiber texture [note, for example, that the brightest ring results from (220) reflections and that the (111) and (200) rings are almost completely absent]. In addition, the film contains a significant population of grains with random in-plane orientations, as well as a significant population of as-deposited epitaxially aligned grains.

Figure 4(b) shows a film that has been deposited at room temperature and then subsequently annealed *in situ* at 500 °C for 3 h. Comparison of Figs. 4(a) and 4(b) shows that there is clearly a substantial increase in the average grain size to over 1 μm after annealing. Also, there has been an evolution in the orientation of the film as indicated by the representative TED pattern. Specifically, the in-plane orientation has become much more restricted, indicating that those grains which dominated during grain growth had preferred epitaxial orientations. The uniformity of the dark-field image in Fig. 4(b) also shows that nearly all the misoriented grains have been consumed. X-ray pole figure analyses of the Au on mica films generally support the TED results reported above. The as-deposited film $(111)_{Au}$ pole figures indicate that the grains which are epitaxially aligned initially have the (111)Au‖(001)mica, [1$\bar{1}$0]Au‖[010]mica orientation. However, after annealing and epitaxial grain growth, the film consists mostly of epitaxial grains with (111)Au‖(001)mica, [2$\bar{1}\bar{1}$]Au‖[010]mica orientations. Only a small fraction of the grains retain the as-deposited (111)Au‖(001)mica, [1$\bar{1}$0]Au‖[010]mica orientation. (Note that these grains were not detected using TED of the annealed film, due to the limited area measured.) Thus, after epitaxial grain growth of Au on mica, a different orientation than that favored in the as-deposited film grows preferentially. In the notation above (*lmn*)Au‖(*xyz*)mica indicates the fiber texture, i.e., which planes in the film and substrate are parallel, and [*lmn*]Au‖[*xyz*]mica indicates the in-plane orientation, i.e., which in-plane directions in the film and substrate are parallel. These results for Au on mica clearly demonstrate that epitaxial grain growth has occurred. It is also interesting to note that in this case the low misfit orientation does not dominate during epitaxial grain growth.

In the film shown in Fig. 4(b) there remain grain boundaries due to the fact that all the grains are not uniformly aligned. However, most of the grain boundaries are low-angle boundaries, with predominantly tilt components of less than 20°, as estimated from the elongation of the (220) diffraction spots. Other than grain boundaries, the films have relatively low defect densities and are fully continuous.

Figure 4(c) shows a 650-Å-thick Au film deposited on mica directly at 400 °C, so that conventional epitaxy has occurred. While this film is epitaxial, it is not fully continuous, and it has a significantly higher density of dislocations and grain boundaries than the film obtained by epitaxial grain growth, shown in Fig. 4(b). Films deposited at temperatures higher than 400 °C were even less continuous and more

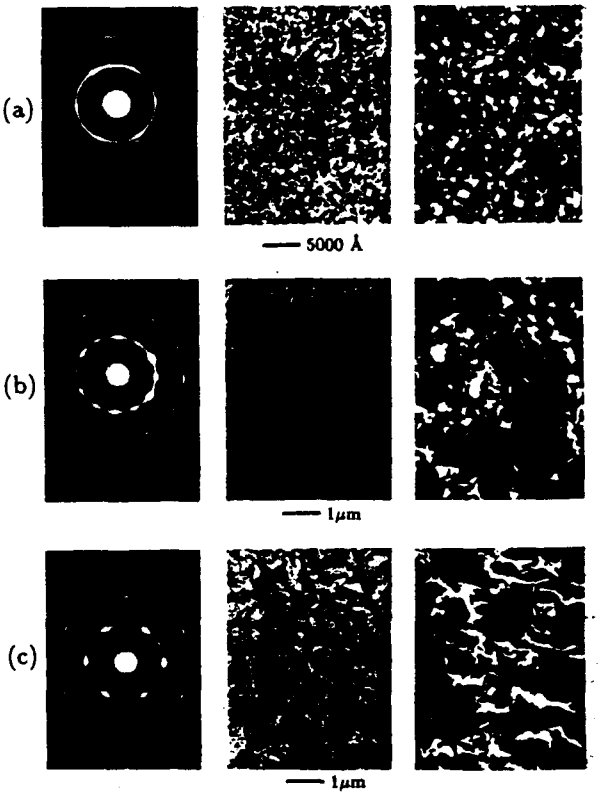

FIG. 5. Transmission electron diffraction patterns (left), bright-field TEM micrographs (center), and dark-field TEM micrographs (right) of 650-Å-thick Al films, (a) as-deposited on vacuum-cleaved (001) mica at room temperature, (b) deposited at room temperature and *in situ* annealed for 3 h at 360 °C, and (c) deposited at room temperature and annealed *in situ* for 3 h at 500 °C.

poorly aligned. As discussed in Sec. V, this is due to the higher deposition temperatures required for conventional Volmer–Weber epitaxy. Very thin (<650 Å), fully continuous films cannot be obtained for deposition temperatures at or above 400 °C. However, in Volmer–Weber epitaxy, low defect densities cannot be obtained at or below 400 °C.

Figure 5 shows TED patterns, bright-field TEM micrographs, and dark-field TEM micrographs for 650-Å-thick aluminum films deposited on vacuum-cleaved mica. Figure 5(a) shows the as-deposited film at room temperature. The TED pattern indicates near-uniform (111) fiber texture and a distribution of in-plane orientations similar to that observed in the as-deposited Au films on mica, except with a subpopulation of grains with (111)Al‖(001)mica, [1$\bar{1}$0]Al‖[010]mica epitaxial alignments.

As shown in Fig. 5(b), after *in situ* annealing for 3 h at 360 °C, grain growth has occurred and has resulted in a new significant subpopulation of (111)Al‖(001)mica, [2$\bar{1}\bar{1}$]Al‖[010]mica epitaxially aligned grains. This result clearly suggests that there are *two* in-plane orientations that lead to surface and interface energy minimization. X-ray analysis indicates a similar result for Au on mica.

Figure 5(c) shows an Al film that was deposited at room temperature and then *in situ* annealed for 3 h at 500 °C. In this case, further grain growth and evolution of grain ori-

TABLE I. Orientation before and after epitaxial grain growth.

System	Orientation	Misfit (%)	Comments
Au on mica	(111)film‖(001)sub.	− 3.7	Dominant as-deposited
	[1$\bar{1}$0]film‖[010]sub.[a]		reduced after EGG
	(111)film‖(001)sub.	+ 11.2	Present as-deposited,
	[2$\bar{1}\bar{1}$]film‖[010]sub.[a]		dominant after EGG
Al on mica	(111)film‖(001)sub.	− 4.4	Dominant as-deposited
	[1$\bar{1}$0]film‖[010]sub.[b]		and after EGG
	(111)film‖(001)sub.	+ 10.4	Present as-deposited,
	[2$\bar{1}\bar{1}$]film‖[010]sub.[b]		reduced after EGG
Cu on mica	(111)film‖(001)sub.	− 14.8	Present as-deposited
	[1$\bar{1}$0]film‖[010]sub.[b]		reduced after EGG
	(111)Au‖(001)mica	− 1.7	Present as-deposited,
	[2$\bar{1}\bar{1}$]film‖[010]sub.[b]		dominant after EGG
Au on NaCl, KCL,	(001)film‖(001)sub.	− 27.5, − 35.1	As-deposited and
KBr	[100]film‖[100]sub.	− 38.0	conventional epitaxy
	(001)film‖(001)sub.	+ 2.5, − 8.3	Never observed
	[100]film‖[110]sub.	− 12.4	
	(111)film‖(001)sub.	− 27.5,35.3	Present as-deposited,
	[1$\bar{1}$0]film‖[110]	− 35.1	dominant after EGG

[a] Determined by x-ray pole figure.
[b] Determined by TED.

entations has occurred, resulting in the apparent dominance of grains with (111)Al‖(001)mica, [1$\bar{1}$0]Al‖[010]mica epitaxial orientations. This result suggests that the [1$\bar{1}$0]Al‖[010]mica orientation dominates in competitive growth among *epitaxially* aligned grains. The orientation that grows preferentially has smaller misfit than the orientation being consumed (see Table I).

Figure 6 shows TED patterns, bright-field TEM micrographs, and dark-field TEM micrographs of 650-Å-thick Au films deposited on vacuum-cleaved (100) surfaces of NaCl. Figure 6(a) shows the as-deposited film at room temperature, and Fig. 6(b) shows the results of epitaxial grain growth that occurred during a 3-h *in situ* anneal at 325 °C. From the diffraction pattern in Fig. 6(a) it can be seen that the as-deposited film contains significant populations of grains with several different orientations, notably (001)Au‖(001)NaCl, [100]Au‖[100]NaCl and (111)Au‖(001)NaCl, [1$\bar{1}$0]Au‖[110]NaCl (as well as [1$\bar{1}$0]Au‖[1$\bar{1}$0]NaCl, which is symmetrically equivalent). The grains of the first orientation, illuminated in the dark-field image of Fig. 6(a), are quite numerous and very small. The much larger grains seen in the bright-field image of Fig. 6(a) almost all have restricted (111) texture (i.e., the second orientation mentioned above) and thus are not illuminated in the {200} dark-field image. Note that the NaCl surface normal is parallel to an axis of fourfold symmetry in the NaCl. It is therefore not surprising that the as-deposited film has a subpopulation of grains with similarly aligned directions with fourfold symmetry, specifically, grains with (001)Au‖(001)NaCl, [100]Au‖[100]NaCl epitaxial orientations. What *is* surprising is that after epitaxial grain growth there is a near-uniform (111) fiber texture and a dominant subpopulation of (111)Au‖(001)NaCl, [1$\bar{1}$0]Au‖[110]NaCl epitaxial grains so that the surviving epitaxial orientation has a surface normal with threefold symmetry and the fourfold symmetric orientation has been eliminated. Clearly minimization of the total energy of the film, in this case, does not require lattice marching.

It should be noted that in contrast with these results for epitaxial grain growth, films that were deposited directly at 250 °C, so that conventional epitaxy occurred, exhibit uni-

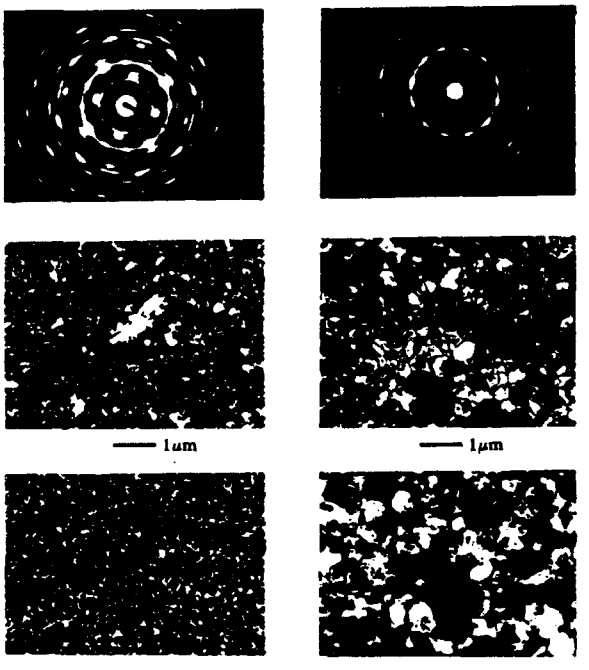

FIG. 6. Transmission electron diffraction patterns (upper), bright-field TEM micrographs (center), and dark-field TEM micrographs (lower) of 650-Å-thick Au films (a) as-deposited on vacuum-cleaved (001) NaCl and (b) deposited at room temperature and *in situ* annealed for 3 h at 325 °C.

form (001)Au||(001)NaCl, [100]Au||[100]NaCl epitaxial alignment. Mader, Feder, and Chaudhari[21] showed that epitaxial (001) Au films can recrystallize to a (111) orientation during annealing after removal from NaCl substrates. This result suggests that the (111) orientation minimizes the energy of the free surface of a Au film. This conclusion, combined with the results reported here, suggests that the free surface plays an important role in determining the energy-minimizing epitaxial orientation resulting from grain growth in Au on NaCl and specifically that $\{\gamma_i[(111)\text{Au}/(001)\text{NaCl}] + \gamma_s[(111)\text{Au}]\} < \{\gamma_i[(001)\text{Au}/(001)\text{NaCl}] + \gamma_s[(100)\text{Au}]\}$. It might generally be expected that for fcc metals γ_s will be larger than γ_i. Therefore, (111) epitaxial orientations might also result from epitaxial grain growth in other systems, even if γ_i is minimized by grains with textures other than (111).

The results described above, as well as additional results for other systems, are summarized in Table I. From these results it can be seen that epitaxial grain growth has been observed in a variety of systems. Results for Au on KCl and KBr are similar to the results for Au on NaCl and results for Cu and Ag on mica are similar to the results for Au and Al on mica, in that epitaxial grain growth leads to dominance of one or two specific low energy orientations.

V. DISCUSSION, SUMMARY, AND CONCLUSIONS

The results presented above clearly demonstrate that grain growth in polycrystalline films deposited on single-crystal substrates can lead to the dominance of grains with epitaxial orientations. This is true even in the absence of good film-substrate lattice matching and should therefore be true in a wide variety of materials.

As demonstrated in the case of Au on mica, under some circumstances epitaxial grain growth can lead to epitaxial films with greater crystalline perfection than conventional epitaxy. This is especially true in very thin epitaxial films. In general, for films that grow by the Volmer–Weber mechanism, the average island spacing during deposition increases with increasing substrate temperatures. The minimum thickness required for film continuity therefore increases with increasing deposition temperature. Unfortunately, uniform epitaxial alignment of nuclei or discrete islands generally requires deposition at elevated temperatures. There is therefore a minimum film thickness for which Volmer–Weber epitaxy can be used. In contrast, in epitaxial grain growth, films can be deposited at arbitrarily low temperatures because initially polycrystalline films are desired. Therefore very thin continuous films can be obtained and are in fact preferred in order to enhance the importance of surface and interface energy minimization, as indicated by Eq. (5).

Finally, as most clearly demonstrated by the results obtained for Au on NaCl, epitaxial grain growth can lead to films with different ultimate epitaxial orientations than are obtained by conventional epitaxy. This probably is due, at least in part, to the fact that epitaxial grain growth leads to minimization of the total energy of a film, which requires reduction of the energy of the top surface of the film as well as the energy of the film-substrate interface. In conventional Volmer–Weber epitaxy, energy minimization occurs at the nucleation or island-growth stages, when the geometric form of the deposited material is fundamentally different. Epitaxial grain growth therefore provides a fundamentally different alternative to conventional Volmer–Weber epitaxy and a new means of obtaining and studying epitaxial films.

ACKNOWLEDGMENTS

We would like to thank Hai P. Longworth for assistance with the x-ray analysis. This work was supported by the Air Force Office of Scientific Research through Grant No. AFOSR-85-0154 and by MIT's Joint Services Electronics Program through Grant No. DAAL03-89-C-0001. J. Floro has also been supported by an AT&T Fellowship.

[1] J. C. Bean, Appl. Phys. Lett. **36**, 741 (1980).
[2] F. C. Frank and J. H. van der Merwe, Proc. R. Soc. London Ser. A **198**, 205 (1949).
[3] M. Volmer and A. Weber, Z. Phys. Chem. **119**, 227 (1926).
[4] J. A. Venables and G. L. Price, in *Epitaxial Growth*, edited by J. W. Matthews (Academic, New York, 1975), Part B, p. 382.
[5] A. Masson, J. J. Metois, and R. Kern, in *Advances in Epitaxy and Endotaxy*, edited by Helmut Gunther Schneider and Volker Ruth (VEB Deutscher Verlag fur Grundstoffindustrie, Liepzig, 1971), p. 103.
[6] C. V. Thompson, Acta Metall. **36**, 2929 (1988).
[7] H. Pascard, C. Quintana, F. Hoffman, and C. Sella, J. Cryst. Growth **13/14**, 225 (1972).
[8] M. Hillert, Acta Metall. **13**, 227 (1965).
[9] D. Turnbull, Trans. Am. Inst. Min. (Metall.) Eng. **191**, 661 (1951).
[10] C. V. Thompson, J. Appl. Phys. **58**, 763 (1985).
[11] C. V. Thompson and H. I. Smith, Appl. Phys. Lett. **44**, 603 (1984).
[12] J. E. Palmer, C. V. Thompson, and H. I. Smith, J. Appl. Phys. **62**, 2492 (1987).
[13] H. J. Kim and C. V. Thompson, J. Appl. Phys. **67**, 757 (1990).
[14] P. A. Beck, M. L. Holtworth, and P. R. Sperry, Trans. Am. Inst. Min. (Metall.) Eng. **180**, 163 (1949).
[15] C. C. Wong, H. I. Smith, and C. V. Thompson, Appl. Phys. Lett. **48**, 335 (1986).
[16] G. Wulff, Z. Kriustallogr. Min. **34**, 449 (1901); C. Herring, in *Structures and Properties of Solid Surfaces*, edited by R. Gomer and C. S. Smith (University of Chicago, Chicago, 1953), p. 5.
[17] J. W. Cahn and J. E. Taylor, *Phase Transformations '87* (British Inst. of Metals, London, 1988), p. 545.
[18] H. Jaeger, P. D. Mercer, R. G. Sherwood, Surf. Sci. **13**, 349 (1969).
[19] J. W. Matthews, Philos. Mag. **12**, 1143 (1965).
[20] H. Jaeger, P. D. Mercer, and R. G. Sherwood, Surf. Sci. **6**, 309 (1967).
[21] S. Mader, R. Feder, and P. Chaudhari, Thin Solid Films **14**, 63 (1972).